Journal of Food Engineering 120 (2014) 248–259

Contents lists available at ScienceDirect

Journal of Food Engineering

journal homepage: www.elsevier.com/locate/jfoodeng

In situ quality assessment of intact oil palm fresh fruit bunches using rapid portable non-contact and non-destructive approach

Muhammad Makky [a,b], Peeyush Soni [a,*]

[a] Agricultural Systems & Engineering, SERD, Asian Institute of Technology, Pathumthani 12120, Thailand
[b] Department of Agricultural Engineering, Andalas University, Padang 25163, West Sumatera, Indonesia

ARTICLE INFO

Article history:
Received 2 May 2013
Received in revised form 22 July 2013
Accepted 5 August 2013
Available online 14 August 2013

Keywords:
Oil palm
FFB
VIS/NIR spectroscopy
Nondestructive
Ripeness
OC
FFA

ABSTRACT

The oil palm (*Elaeis guineensis* Jacq.) fresh fruits bunch (FFB) quality can be determined by its ripeness, oil content (OC) and free fatty acid (FFA) level. The change in fruit's color upon ripening due to biochemical reactions can be observed through VIS/NIR spectroscopy. In this study, portable VIS/NIR spectrometer was employed to rapidly measure quality of oil palm FFB on-site, by means of non-contact and non-destructive approach. A mean-normalized method was used in pre-processing the bunch's spectral reflectance data within 400–1000 nm range using 10 nm intervals. Two statistical analyses are performed to models FFB quality. First, a forward-stepwise method is employed to establish multiple linear regressions (FS-MLR), and second, a combination between principal component analyses with multilayer perceptron neural network (PCA–MLP). These statistical analyses are employed for predicting the FFB ripeness, OC and FFA. Performances of best models were demonstrated by coefficient of determination (R^2), standard error of calibration (SEC) and standard error of prediction (SEP), which were respectively 0.9688, 0.1782, 0.4258 for ripeness prediction, 0.984, 0.25085, 0.4366 for OC prediction, and 0.9909, 0.0917, 0.2367 for FFA prediction model. The application of FS-MLR method for modeling the FFB quality delivered better performances, since it introduced more predictor variables.

1. Introduction

The oil palm industry in Indonesia significantly contributes to its economy by employing millions of people. Indonesia supplies more than 45% of the global demand. With 7.8 million hectares of plantations and production surpassing 23 million tons of palm oil annually (Makky and Soni, 2013a, 2013b), Indonesia becomes the largest palm oil producer. Indonesian oil palm industry needs to increase their high quality palm oil production while keeping the production costs low in order to maintain its competitive advantages (Makky et al., 2004). This edible oil is extracted from its fleshy mesocarp by means of mechanical extraction (Makky et al., 2012). The fruit's quality can be determined by its ripeness, oil content (OC) and free fatty acid (FFA) level, that eventually determine the quality of the palm oil produced. In practice, manual ripeness assessment is carried out by visual inspection, while fruit's oil content and oil's free fatty acid level are determined through laboratory chemical analysis. These methods are time consuming, labor intensive and prone to human error. In addition to being costly, laboratory chemical analysis is usually performed to only a few samples and requires destructive sampling. Furthermore, it takes time to obtain the results and therefore poses challenge to the industries. It is necessary to replace these methods with rapid and non-destructive as well as cost-efficient techniques.

As the fruits ripe, its surface color gradually changes due to biochemical reactions in the fruits. The color changes due to variation in carotenoids and chlorophyll pigments ratios in its skin (Ikemefuna and Adamson, 1984), and can be correlated to fruit ripeness level. The chlorophyll is known to be highest in raw fruits, and gradually decreases along with ripening fruit. In contrast, the carotenoid is low in raw fruits and gradually increases during ripening process (Ikemefuna and Adamson, 1984). Therefore, it is possible to measure the ripeness of oil palm fruits or bunches by measuring the ratio of chlorophyll to carotenoids, or vice versa, in fruit skin. This condition is observable through spectral reflectance analysis, and hence the spectroscopy suits the assessment requirements. The advantage of VIS/NIR spectroscopy has been described as being low cost, low maintenance and chemical-free process while providing short measuring time with limited sample preparation (Valous et al., 2010). Another advantage of the technique is that it facilitates a continuous quality evaluation of the object. Using visible and near infrared spectrum, spectroscopy analysis can obtain internal properties of fruits and produces result in rapid and non-destructive manner.

The use of VIS/NIR spectral analysis to assess agricultural products' quality as a rapid and non-destructive technique has

* Corresponding author. Tel.: +66 2 524 5480; fax: +66 2 524 6200.
E-mail addresses: muh_makky@yahoo.com (M. Makky), soni.ait@gmail.com (P. Soni).

0260-8774/$ - see front matter © 2013 Elsevier Ltd. All rights reserved.
http://dx.doi.org/10.1016/j.jfoodeng.2013.08.011

increased recently (Magwaza et al., 2012; Bertone et al., 2012). Spectroscopy analysis both in visible and near infrared range, has been widely used for classification as well as assessing quality and internal properties of fruits such as apple (Bertone et al., 2012), blueberries (Sinelli et al., 2008), jujubes (Wang et al., 2010), mandarin (Magwaza et al., 2012), mango (Subedi et al., 2007), tomato (Shao et al., 2007; Sirisomboon et al., 2012), pear (Fu et al., 2007), and plum (Louw and Theron, 2010; Pérez-Marín et al., 2010). This method is well known as a rapid and non-destructive analysis for assessing fruit quality. Nevertheless, among these researches, oil palm fruits receive lack of attention. No research has been reported for studying physical appearance of FFB and its internal properties using VIS/NIR spectroscopy under actual field operation.

The objective of this study was to use VIS/NIR spectroscopy for measuring ripeness and internal quality of oil palm fruits. The specific objectives were to analyze relationships between VIS/NIR spectral reflectance characteristics and three important oil palm fruit quality indices (ripeness fraction, OC and FFA level) assessed through manual visual inspection and laboratory chemical analysis. The FFA level determines the quality of palm oil, because the presences of high FFA result in poor quality oil. Another advantage of low level FFA is less chemical processing, thus saving production cost and promoting green and more environmental friendly production in oil palm industries. These correspond to the requirements of palm oil industries where greater volume of quality production is desirable, through maximizing output from the oil content in the fruits, while minimizing its FFA level.

2. Material and methods

2.1. Samples preparation

The oil palm FFBs were harvested from 7 to 20 year-old trees during June–July, 2011 at National Plantation Company's Kertajaya plantations, Banten Province, Indonesia. All plants were of tenera variety, and the FFBs were harvested from eight different ripeness fraction conditions (Table 1), according to Indonesian Oil Palm Research Institute (IOPRI) standard (IOPRI, 1997). Every ripeness fraction has distinguished properties, including the fruit color and the number of detached fruitlets (Fig. 1). The FFBs' samples were classified by a panel of three experienced graders using visual assessment. In this research, 96 FFB samples, 12 from each ripeness fraction, were used to be analyzed by spectrophotometry. Infected, bruised or damaged bunches were discarded before these bunches with good appearance were selected. All containments on the bunch such as dirt, fiber and leaves were removed before measurement performed.

Since changes in color of oil palm fruits can be distinguished during fruit ripening process, due to the change of chlorophyll and carotenoids pigment concentrations in the fruits, measurement of spectral reflectance were performed in order to determine the change in these two pigments' ratio. Within a bunch, the color of the fruitlets is usually not uniform, and there exists gradation of fruitlets color from the top part of the bunch (apical) to the bottom part of the bunch (basal). Therefore, the measurements were performed at the three parts of each bunch, i.e. apical, middle and basal part. Subsequently, measurements were replicated thrice for each part, located around the equator, with the distance of about 120° apart (Fig. 2a).

In this study, the nigrescens fruit type was selected being the major fruit type popularly grown in Indonesia. As described by Corley and Tinker (2003), these fruits can be distinguished by its purplish black color at the apex and pale greenish yellow color at the base during raw or unripe state. Bunches were inspected on site. For each bunch, measurement and data acquisition took less than one minute, and then the bunch was immediately sent to the laboratory for chemical analysis.

Table 1
FFB ripeness fraction classification (IOPRI, 1997).

Ripeness fraction	Quality	Detached fruitlets
F00	Bad	None
F0	Low	Up to 12.5% of outer fruits
F1	**Preferable**	**12.5–25% outer fruits**
F2	**Preferable**	**25–50% outer fruits**
F3	**Preferable**	**50–75% outer fruits**
F4	Low	75–100% outer fruits
F5	Bad	Inner fruits start to detached
F6	Worst	Most fruits detached

2.2. VIS/NIR reflectance spectra measurements

The spectroscopy measurements were performed using Ocean Optic USB2000+VIS–NIR series spectrometer (Ocean optics, USA). The device provided spectral information between 350 and 1000 nm with resolution of 1.5 nm. For the light source, HL-2000 tungsten halogen light sources (Ocean optics, USA) were used. For measuring the reflectance of oil palm fruits surface, optical fiber reflection Probes (QR600-7-VIS–NIR, Ocean optics, USA) were employed to record diffuse or specular reflectance. The reflection probes were coupled to the spectrometer and light source to measure reflection. To calibrate the spectrometer, a white reflec-

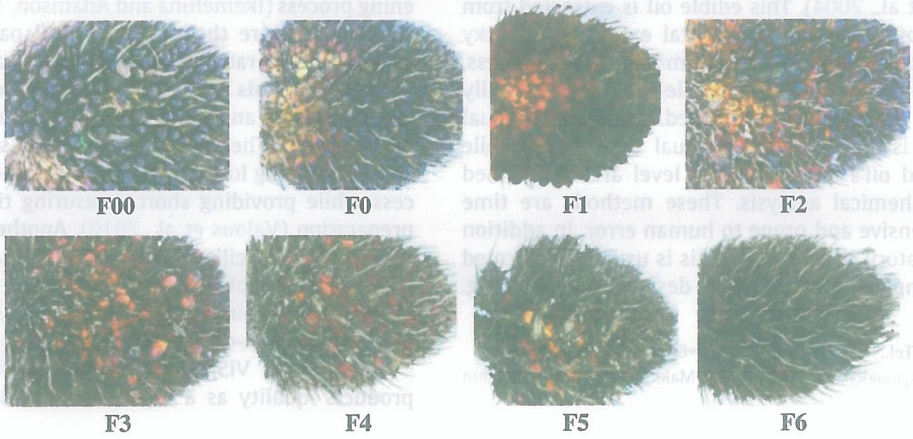

Fig. 1. FFB appearance of different ripeness conditions.

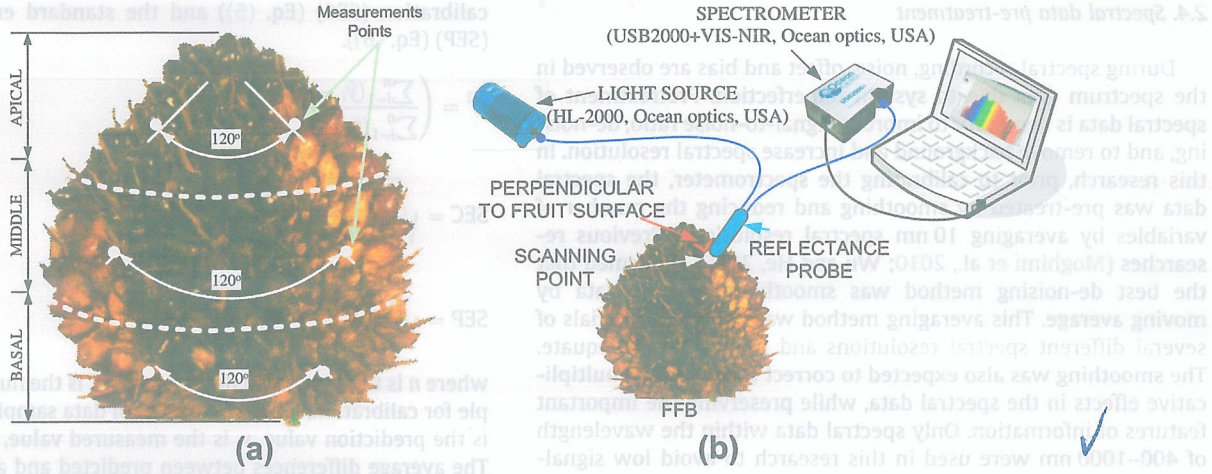

Fig. 2. (a) Measurement positions around equator for basal, middle and apical part of FFB, and (b) experimental setup.

tance standard with spectralon was used (WS-1-SL, Ocean optics, USA).

To overcome electrical noise due to light exposure onto the spectrophotometer, a dark correction was performed by turning off the light source and placing the probe's end with an opaque cap. The calibrated reflectance was calculated as percentage of the reflection of a standard reference material. Immediately, after each bunch measurement, the spectrometer was recalibrated and dark correction was repeated to remove the temperature influence on the equipment. Throughout the measurements, the ambient temperature varied between 27 °C in the morning and 33 °C in the noon.

Each spectrum measurement is recorded as an average of 10 scans. Recorded signals are pre-processed with a completely modular, Java-based spectroscopy software platform that operates on Windows operating systems (SpectraSuite, Ocean optics, USA). The software interfaces with and controls the spectrometer and device with different acquisition parameters, and provides graphical and numeric representations of reflectance spectra data from spectrometer, and also calculates and corrects non-unity for reflection measurements, while displaying *x*-axis data in nanometers.

For each bunch of oil palm fruit, the reflectance spectral measurements were taken at nine different points (Fig. 2a) and the average of these spectra was calculated. Each point measurement was repeated three times and averaged to minimize error in result. In total, 2592 reflectance spectra data were collected from all samples. Experimental set up is described in Fig. 2b. While measuring, the reflectance probe was placed perpendicularly with the fruit surface in order to prevent ambient light reaching the sensor.

The visible and near-infrared reflectance spectra were acquired directly after the bunch harvested. This to ensure the bunch in fresh condition and reduce the effect of free fatty acid formation in mesocarp due to lipase enzyme activities that accelerate after the bunch was harvested (Henderson and Osborne, 1991). To avoid a low signal-to-noise ratio, only the waveband 400 nm to 1000 nm was considered in the calculations.

2.3. Quality parameters measurement

After spectral measurement, each bunch was taken to laboratory for analyzing the oil content and its FFA level. Upon arrival, the samples were boiled immediately to inactivate the lipases. The tests were conducted within 24 h after the bunch had been harvested. Fruitlets were detached from the bunch, and chopped to separate fruit's mesocarp. Mesocarp was weighed using analytical balance (Sartorius, BP 160 P, Germany). Samples were then dried to remove physical water from the mesocarp. The oil in the mesocarp was extracted using soxhlet extractor, with hexane as chemical solvent. The remaining fiber and the oil solution in the thimble were dried to remove the dissolved hexane, and then cooled in the desiccator. It was then weighed in the analytical balance, and the result was recorded for mesocarp oil content calculation. This gravimetric procedure was defined by IOPRI (IOPRI, 1997) in accordance with standards established by the National Standardization Body of Indonesia SNI- 01.2891.1991 (NSAI, 2006). The mesocarp oil (Oil_m) can be calculated as:

$$\%Oil_m = \frac{W_1 - W_2}{W_3} \times 100\% \quad (1)$$

where W_1 is timble and residue weight (g); W_2 is empty timble weight (g); and W_3 is mesocarp sample weight (g).

The CPO recovery from the sample FFB was calculated using equation:

$$\%\text{Oil Content (OC)} = \frac{\sum^{M_f}}{M_{FFB}} \%.M_m \%.Oil_m \quad (2)$$

where M_{FFB} is weight of FFB (kg); M_f is Fruitlets weight (kg);% M_m is percentage of mesocarp weight from fruitlets (%); and % Oil_m is percentage of mesocarp oil (%)

Free fatty acid was considered as an important quality parameter for CPO. FFA was formed as the process of oil hydrolysis to become acid. Accelerated by light and heat, FFA formed in CPO decreases the smoking point, and responsible to undesirable flavors and aroma (Osawa et al., 2007). FFA in the oil was measured by titration. The percentage of FFA in CPO was calculated as palmitic acid and interpreted as the weight of KOH (in miligrams) required to counteracting acid from 1 g of sample. In this research, FFA was measured using the procedure defined according to SNI 01-2901-2006 (NSAI, 2006). This procedure meets the qualification according to the AOCS (American Oil Chemist's Society) official method Ca 5a-40 (AOCS, 2004).

The percentage of FFA (as palmitic) is expressed as:

$$\%\text{ FFA (as palmitic)} = \frac{25.6NV}{W} \quad (3)$$

where V is volume of KOH (ml); N is titration solution normalization; W is sample weight (g); and 25.6 is constant (to calculate FFA as palmitic acid).

2.4. Spectral data pre-treatment

During spectral recording, noise, offset and bias are observed in the spectrum data due to system imperfection. Pretreatment of spectral data is necessary to improve signal-to-noise ratio, de-noising, and to remove background and increase spectral resolution. In this research, prior to calibrating the spectrometer, the spectral data was pre-treated by smoothing and reducing the number of variables by averaging 10 nm spectral resolutions. Previous researches (Moghimi et al., 2010; Wu and He, 2006) confirmed that the best de-noising method was smoothing spectral data by moving average. This averaging method was chosen after trials of several different spectral resolutions and found to be adequate. The smoothing was also expected to correct additive and multiplicative effects in the spectral data, while preserving the important features of information. Only spectral data within the wavelength of 400–1000 nm were used in this research to avoid low signal-to-noise ratio.

2.5. Forward stepwise multiple linear regression (FS-MLR) model

Multiple linear regression (MLR) analysis is widely used for calibrating reflectance visible – near infrared spectral analysis model (Liu et al., 2008). Since the samples in this research were less than the variables of VIS/NIR spectra data, it was not possible to directly establish the MLR mode (Naes and Mevik, 2001) due to collinearly. A forward stepwise method was employed to improve model accuracy and efficiency by removing collinearity of variables. This algorithm improved the prediction accuracy by using less variables compared to conventional MLR model. The Forward Stepwise MLR model was built using statistical engineering software (IBM, USA). The FS-MLR prediction models were constituted of several reflectance wavelength segments. Although it is precarious to determine the importance of each wavelengths segment due to collinearity problems, the exegesis of the model remain possible.

2.6. Principal component analysis with multilayer perceptron neural network (PCA–MLP) models

In this study, the principal component analysis (PCA) is used to explain the variance in the spectral data. This analysis was performed by transforming data of spectral variables uncorrelated linearly into a novel coordinate system, which gave the greatest variance of data on the consecutive coordinates (Jolliffe, 2002). The PCA removed spectral data variables that had redundancy, distinguished with strong correlation with one another. The principal components have much smaller variable numbers, yet still provide information for most of the variance in the observed spectral variables.

By utilizing obtained principal components as input predictor's variables, Multilayer perceptron neural network (MLP) models were built using statistical engineering software (IBM, USA). The MLP models were used for approximation estimation of FFB qualities (i.e. ripeness, OC and FFA). This procedure was done by training a set of multilayer perceptron, hidden layers and output layer. To ensure models did not over fit upon training and performed poorly upon validation, the number of hidden layers and processing elements were set to be changed automatically by statistical software.

2.7. Model evaluation

The model performance was evaluated by comparing the prediction results and measured values, in the validation sets. The main performance statistics used for model validation were the coefficient of determination (R^2) (Eq. (4)), the standard error of calibration (SEC) (Eq. (5)) and the standard error of prediction (SEP) (Eq. (6)).

$$R^2 = \left(\frac{\sum_{i=1}^{n}(\hat{y}_i - y_i)^2}{\sum_{i=1}^{n}(\hat{y}_i - y_m)^2}\right) \tag{4}$$

$$\mathrm{SEC} = \sqrt{\frac{\sum_{i=1}^{n_c}(\hat{y}_i - y_i)^2}{(n_c - 1)}} \tag{5}$$

$$\mathrm{SEP} = \sqrt{\frac{\sum_{i=1}^{n_v}(\hat{y}_i - y_i - bias)^2}{(n_v - 1)}} \tag{6}$$

where n is the number of data sample, n_c is the number of data sample for calibration, n_v is the number of data sample for validation, $\hat{y}_i$ is the prediction value, y_i is the measured value, y_m is mean value. The average differences between predicted and actual values were considered as bias (Eq. (7)).

$$bias = \left(\frac{\sum_{i=1}^{n_v}(\hat{y}_i - y_i)}{n_v}\right) \tag{7}$$

The performance of the model on calibration was highly related to the SEC results while upon validation, the SEP results confirmed the validation of the model. The coefficients of determination (R^2) were used both in calibration (R_c^2) and validation (R_v^2) process. The model was considered appropriately accurate when R^2 value was high while SEC and SEP values were low. Another criterion for model acceptance was having small differences in the value of SEC and SEP; since it indicates that model calculated minimum latent variables and noises are not modeled.

Samples were divided into calibrations and cross-validations data sets, and distribution of data covered the same range of ripeness fraction, oil content and free fatty acid results. In order to increase model performance, the spectral reflectance data were pre-processed as described in the previous section. Out of 96 samples, 2/3 ($n_c = 64$) of the data were used for calibrating the models, while the rest 1/3 ($n_p = 32$) was used for cross-validations of the models.

3. Results and discussion

The reflectance spectral data retrieved from the measurement were within 340 and 1022 nm. However, in the extreme regions the signal-to-noise ratios are considerably low, and might affect the model accuracy. Therefore, only data ranging within 400 nm and 1000 nm considered to have useful information and were used in the model. This spectral information was employed to generate the model for predictions of ripeness fraction and chemical parameters for each bunch.

Fig. 3a shows original average reflectance spectra of oil palm FFBs measured in each ripeness fraction, within the wavelength range of 400–1000 nm for normal fruits. Even after trimming the outliers, noise in the spectrum data is still present. This initial data from the spectral acquisition was preprocessed. Average mean-normalized reflectance spectra data of 10 nm interval were used for pre-processing, and the result is shown in Fig. 3b.

The relative reflectance data showed that, in general, normal bunch has lower reflectance at lower ripeness fraction compared to higher ripeness bunch. The results reveal clearly distinguishable spectral characteristics for each fraction, especially within the wavelength of 550–700 nm (Fig. 3b).

The differences of reflectance in the visible range can be correlated to the change of color, due to difference of chlorophyll and carotene concentrations in the bunch at each fraction. During ripening, the color of the bunch becomes lighter over time and thus

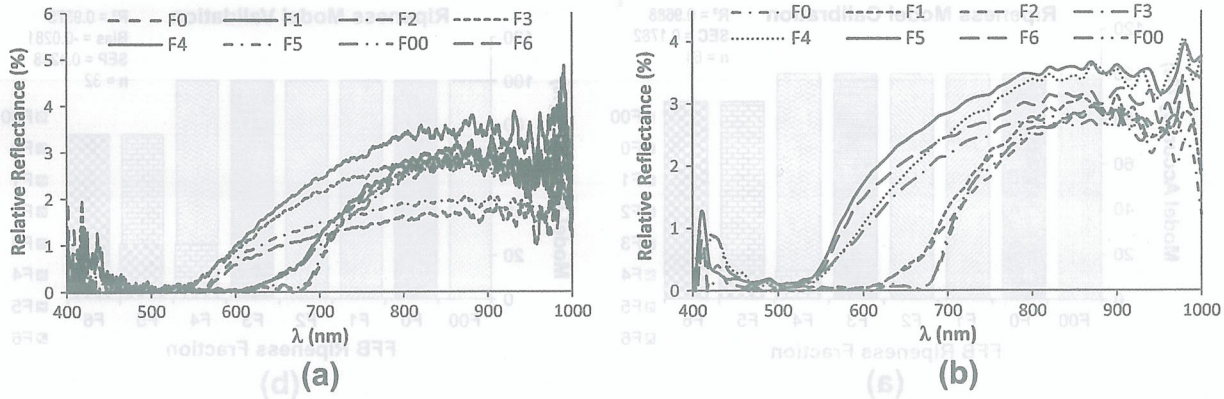

Fig. 3. (a) The average relative reflectance data (%) from each ripeness fraction (F00–F6), and (b) Average mean-normalized reflectance spectra data using 10 nm interval.

Table 2
Ripeness model predictors and correlated coefficients.

No.	1	2	3	4	5	6	7	8	9	Intercept
Coefficients	−0.1442	−1.6285	−2.5154	2.1905	1.4357	−2.7612	0.8597	0.8086	0.1806	3.0567
λ (nm)	400	540	560	590	670	800	910	940	1000	

the reflectance values within the visible range from its surface became higher. Chlorophyll is known to absorb most blue and red light in the visible spectrum, while reflecting green light. Two main types of chlorophyll, namely a and b, are effective photoreceptors and have strong absorption bands in the visible regions of the spectrum with maximum absorbance at 430 and 662 nm for chlorophyll-a, and 453 and 642 nm for chlorophyll-b (Streitweiser, 1981). Carotenoids have absorbance within the visible spectrum of 400 and 500 nm. Referring to the Beer's law, carotenoids' absorbance can be correlated to its concentration, and enables to estimate concentration of carotenoid in a sample. In general, carotenoids can be in the forms of β-carotene, α-carotene, lycopene, β-crytoxanthin, zeaxanthin, or lutein. Researchers have reported differences of carotenoids peak absorbance (Britton et al., 1995) which are α-carotene (422, 445 and 473 nm), β-carotene (425, 450 and 478 nm), β-cryptoxanthin (428, 450 and 478 nm), Lutein (421, 445 and 474 nm), Lycopene (444, 470 and 502 nm), and Zeaxanthin (425, 450, 478 nm). The red color in oil palm fruit is due to the content of red pigment that has been identified as β-carotene, with the absorbance peaks of 444–490 nm (Nde-Aga et al., 2007). However, some researchers have suggested that the carotenes in the palm oil can be determined by spectrophotometry using 446 nm wavelength (Moh et al., 1999).

These known properties of both chlorophyll and carotenoids in oil palm fruits were taken into account for modeling the ripeness and quality parameters of fruits using regression of spectral and chemical analysis data.

3.1. Modeling the FFB ripeness

3.1.1. FS-MLR method for FFB ripeness prediction

Modeling of bunch ripeness using a FS-MLR was done as a statistical analysis by selecting the suitable wavelengths for ripeness estimation. The forward stepwise multiple linear regressions method for creating the model was chosen. In generating the models, the number of predictors to be included was taken into consideration, since too many latent variables result in noise in the model. Optimum number of variables that included in the calculation provided best fit model (highest R^2). Different number of predictors were attempted to achieve highest coefficient of determination (R^2), while keeping number of variables fairly minimum. The numbers of predictors introduced in the model were chosen corresponding to model's coefficient of determinant, which was the highest when the model included nine predictor variables.

Thus, the ripeness prediction model can be written as:

$$F = C + C_1\lambda_1 + C_2\lambda_2 + C_3\lambda_3 + \ldots + C_9\lambda_9 \quad (8)$$

where F is ripeness fraction number, C is constant, C_n is coefficient of nth predictor, and λ_n is the pre-treated reflectance value of the nth predictor. These nine predictors with its coefficient and one constant that introduced in the model are shown in Table 2.

The predictors used in the ripeness model are pre-treated reflectance data at wavelength of 400, 540, 560, 590, 670, 800, 910, 940 and 1000 nm. The variables in the model suggest that significant differences in ripeness can be determined by using reflectance at these wavelengths. In relation to the chlorophyll, the predictor in the model suggests that the chlorophyll-a, with peak absorbance near the 670 nm was contributing in the model, while chlorophyll-b as well as carotenoids were not significantly considered. This result indicated that ripeness model showed a low value of R^2 when calibrating the model with the ratio of chlorophyll to carotenoids. This may also give an impression that modeling for ripeness cannot be simplified by predicting the ratio of chlorophyll to carotenoids alone in the fruits. The wavelength selection in the model, however, deviates from the previous research, where wavelengths of 740, 750 and 760 nm (Junkwon) and 570, 670, 750, and 870 nm (Saeed et al., 2012) were considered for the ripeness.

The model performance was notably higher when compared to previous researches (Saeed et al., 2012; May and Amaran, 2011). The performance of the model calibration was acceptable with R^2 of 0.9688 and SEC of 0.1782. The performance of model validation was also acceptable with R^2 of 0.9375 and SEP of 0.4258. The calibration and validation results are shown in Fig. 4.

Observed misclassification of ripeness fraction of the bunch was occurred in over ripe fractions (F4, F5 and F6) due to their similar resemblance that can be seen in their overlapping reflectance characteristics. However, this may not affect the model application, since the desired ripeness of oil palm bunches to be processed in the mills were within fraction 1 to fraction 3 (Table. 1). Variation

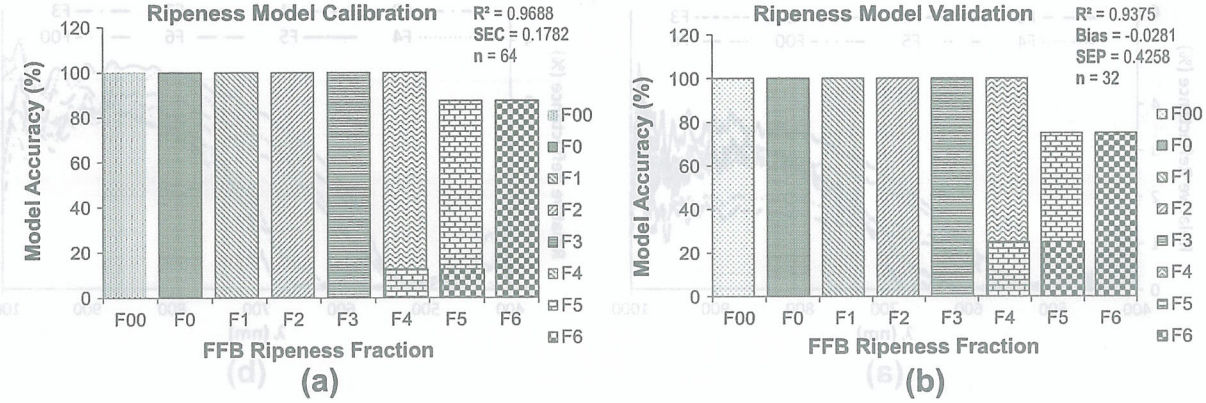

Fig. 4. (a) Calibration and (b) validation results for oil palm FFB ripeness prediction model using FS-MLR method with 9 predictors.

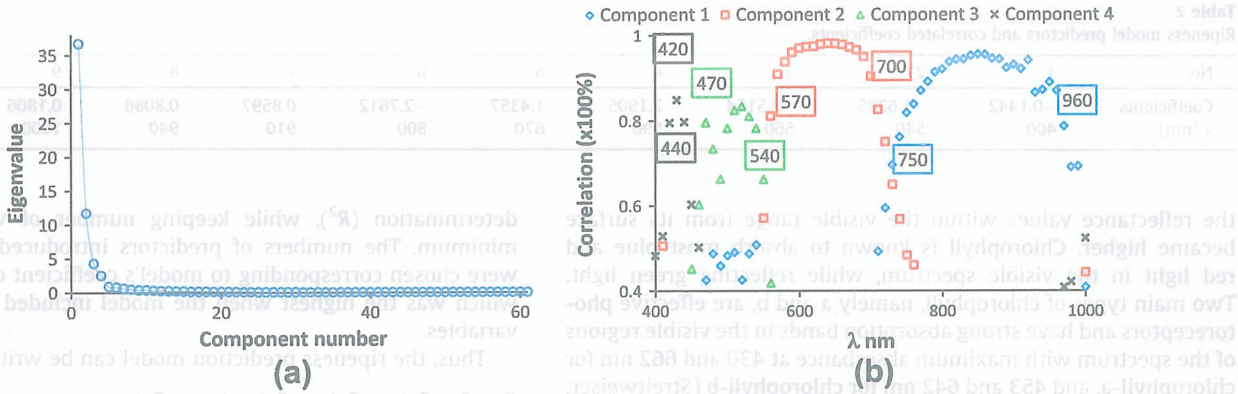

Fig. 5. (a) PCA scree test plot, and (b) correlations of principal components to spectral wavelength.

in regression coefficients with predictors' wavelength for the ripeness prediction of oil palm FFBs are shown in Table 2, where peaks were observed at around 560 nm corresponding to the yellow color, as well as at around 800 nm corresponding to very near infrared.

3.1.2. PCA–MLP method for FFB ripeness prediction

To perform PCA of FFB spectral data, a linear combination of optimally-weighted observed variables are constructed based on correlations among several variables. In general, principal components can be computed by means ofextraction using equation:

$$C_i = b_{i1}X_1 + b_{i2}X_2 + \ldots b_{ip}X_p \quad (9)$$

where C_i is factor score on ith principal component, i is succession number of principal component, b_{ip} is regression coefficient or weight for pth spectral variable for ith principal component, p is succession number of spectral variable, and X_p is the value of pth spectral variable.

The regression coefficient or weight values are predetermined by the statistical software using Eigen-equation. The weights produced by Eigen-equations are the most optimal weights predicted by the software, in such, no other set of value can provide more successfully explained variance in the spectral variables. Although the number of components extracted in this principal component analysis is equal to the number of spectral variables, only the most components that have maximum variance (Eigenvalue >1) are retained, interpreted, and used in MLP analyses.

Initially, 61 components are extracted by PCA, equal to the number of spectral variables being analyzed. Using eigenvalue-one criterion analysis, only four principal components are selected for having eigenvalue greater than 1. This analysis, known as the Kaiser criterion (Kaiser, 1960), is one of the most commonly used criteria for solving the number-of-components to be considered in PCA. In this case, the selection of components using eigenvalue-one criterion analysis provides a confident result since the fourth component displays an eigenvalue of 2.51, which is substantially greater than 1, and the next component (5th) displays an eigenvalue of 0.892, which is clearly lower than 1.

The components selection results agreed with the scree plot test (Fig. 5a), indicated significant distinction between fourth and fifth components. The correlation result between selected principal components and spectral variables is presented in Fig. 5b. Component 1 strongly correlated with spectral reflectance of 750–960 nm, component 2 correlated with spectral reflectance of 570–700 nm, component 3 correlated with spectral reflectance of 470–540 nm, and component 4 correlated with spectral reflectance of 420–440 nm.

The FFB ripeness model developed by means of MLP utilized all four principal components, obtained from processing the spectral data into PCA, as covariates. The statistical software constructed MLP analysis by feed-forward neural network (Fig. 6a), consists of input layer as source neurons, hidden layer as computational neurons, and output layer of computational neurons. Each layer comprised of nodes connected to every node in subsequent layer. The input layer, consists of four principal components as predictor variables and one bias, distributes the inputs to hidden layer. Subsequently, the hidden layer, consists of four variables and one bias, distributes the inputs to output layer. The output layer itself comprised of eight variables, each representing the FFB ripeness. The input signals are propagated in a forward direction on a layer-

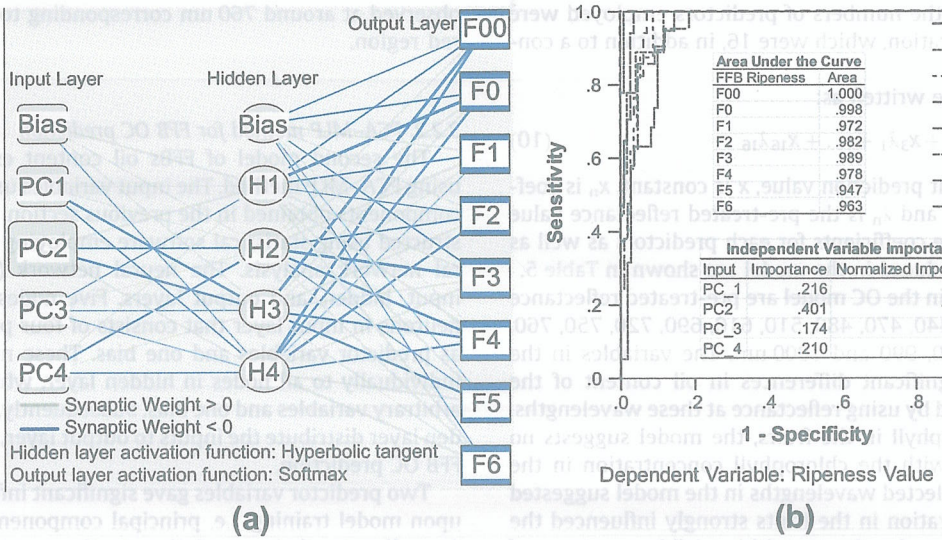

Fig. 6. (a) MLP network diagram of FFB ripeness model, and (b) model performance using ROC analysis.

Table 3
MLP ripeness model summary.

Training	
Cross entropy error	102.27
R^2	0.9393
Stopping rule used	1 Consecutive step(s) with no decrease in error[a]
SEC	0.344
N	64
Testing	
Cross entropy error	71.063
R^2	0.9351
Bias	−0.0853
SEP	0.360
N	32

[a] Error computations are based on the testing sample.

by-layer basis. Receiver operating characteristic (ROC) curve is used to assess model performance (Fig. 6b) upon predicting the FFB ripeness. The area under the curve of ROC graph explains the performance test of the model in the real condition. The FFB model accuracy is measured by the area under the ROC curve. An area of 1 represents a perfect test; an area of 0.5 represents a worthless test. Given the results, the MLP model for assessing FFB ripeness performed exceptionally, particularly upon predicting FFB in Fraction 00 (F00) where area under the curve in the ROC graph obtained a score of 1.

The most importance variable upon model construction is principal component 2 (Fig. 6b), which represents the spectral reflectance variable of 570–700 nm. This suggests that yellow to red color significantly affects the ripeness model, corresponding to the development of FFB color during ripening process. In addition both chlorophyll-a and chlorophyll-b also have strong absorption nature in this wavelength region. The results agreed with FS-MLR ripeness model, where the most significant variable for predicting FBB ripeness is reflectance spectral between 580 to 680 nm (Table 2). The summary of developed model for FFB ripeness prediction using MLP analysis is given in Table 3.

The model coefficient of correlation upon calibration and test are 0.9393 and 0.9351 respectively, with standard error of 0.344 for calibration, and 0.36 for prediction. The R^2 results for FFB ripeness model using PCA–MLP is performed slightly less compared to the model developed using FS-MLR analysis. The composition of FFB ripeness model, established through PCA and MLP methods, is described in the Table 4.

3.2. Modeling FFB's OC

3.2.1. FS-MLR method for FFB OC prediction

Oil in FFB accumulates until its ripening stage. Once the oil palm FFB is cut from the tree, no oil content further develops inside the fruit (Keshvadi et al., 2011). Therefore, the oil content prediction model used the spectral data obtained soon after the bunch harvested. For FFBs oil content estimation using FS-MLR analysis, the model was created by removing non significance variable through stepwise means and *F* statistic. Similarly as previous, in

Table 4
Parameter estimates of FFB ripeness model obtained by PCA–MLP method.

Predictor		Predicted										
		Hidden layer 1				Output layer						
		H(1:1)	H(1:2)	H(1:3)	H(1:4)	F00	F0	F1	F2	F3	F4	F5	F6
Input layer	(Bias)	3.044	.879	.950	−.300								
	PC1_1	.123	.636	−3.049	−.616								
	PC2_1	3.491	−.829	−2.522	1.775								
	PC3_1	−.637	.116	−.433	−.148								
	PC4_1	.571	−1.687	.193	−.446								
Hidden layer 1	(Bias)					−.680	−1.264	1.761	.615	−.698	.222	−.075	−.283
	H(1:1)					−1.261	−7.651	−.908	−.627	2.844	3.373	2.852	3.300
	H(1:2)					1.352	1.574	3.570	−1.159	−4.127	−2.648	−.223	1.849
	H(1:3)					−4.980	1.638	.750	3.320	1.780	−2.118	−2.209	.937
	H(1:4)					−3.381	−2.557	−.096	−2.592	1.858	−1.482	3.374	5.060

generating this model, the numbers of predictors employed were also taken into consideration, which were 16, in addition to a constant value.

The OC model can be written as:

$$OC\ \% = x + x_1\lambda_1 + x_2\lambda_2 + x_3\lambda_1 + \ldots + x_{16}\lambda_{16} \quad (10)$$

where OC% is oil content prediction value, x is constant, x_n is coefficient of nth predictor, and λ_n is the pre-treated reflectance value of the nth predictor. The coefficients for each predictors as well as the constant value introduced in the model are shown in Table 5.

The predictors used in the OC model are pre-treated reflectance data at wavelength of 440, 470, 480, 510, 610, 690, 720, 750, 760, 880, 900, 910, 940, 980, 990 and 1000 nm. The variables in the model suggest that significant differences in oil content of the fruits can be determined by using reflectance at these wavelengths. In regard to the chlorophyll in the fruits, the model suggests no correlation of the OC with the chlorophyll concentration in the fruits. In contrast, theselected wavelengths in the model suggested that carotenes concentration in the fruits strongly influenced the OC, which has common absorbance within visible spectrum of 400 and 500 nm. Previous studies have also revealed that β-carotene is the main carotenoid in the oil palm, and it has been found to have different absorbance peaks. However, the majority of β-carotene in oil palm has the absorbance peak between 440 and 480 nm (Britton et al., 1995; Nde-Aga et al., 2007; Moh et al., 1999), which corroborates to the model in this research. Although the model could not clearly distinguish the β-carotene concentrations in the fruits, it is believed that as the oil forms in the fruit during ripening, the concentration of β-carotene pigment in the oil might vary, thus affecting its spectral characteristics which was reflected in the model's wavelength selection.

The OC prediction model showed acceptable performance both on calibration and validation (Fig. 7). The model's R^2 upon calibration was 0.984 with SEC of 0.25085. While upon validation R^2 value was 0.9891 and SEP of 0.4366. The model was considered appropriate since R^2 value both in calibration and validation were high, while SEC and SEP values were low.

In comparison to the previous studies (Keshvadi et al., 2011; Ismail and Razali, 2010; Hudzari et al., 2009), the developed model performed better for estimating OC in oil palm FFBs. Variation in regression coefficients with predictor's wavelengths for the OC prediction is shown in Table 5, where peaks were observed at around 760 nm corresponding to the very near infrared region.

3.2.2. PCA–MLP method for FFB OC prediction

The second model of FFBs oil content estimation is created using PCA–MLP method. The input variables used are four principal components obtained in the previous section. The model was constructed using statistical software employing a feed-forward neural network analysis. The neural network (Fig. 8a) consists of input, hidden, and output layers. Five nodes are used as source neurons in input layer that consists of four principal components as predictor variables and one bias. These nodes are distributed individually to all nodes in hidden layer, which consists of three arbitrary variables and one bias. Subsequently, all the nodes in hidden layer distribute the inputs to output layer, providing output for FFB OC prediction.

Two predictor variables gave significant influence on the output upon model training, i.e. principal components 1 and 3 (Fig. 8b). According to their correlation to the spectral reflectance data (Fig. 5b), these principal components represent spectral variable wavelength of 470–540 nm and 750–960 nm. The first wavelength spans (470–540 nm) are the area of interest, in which giving indication that there is carotenoids influence for modeling the FFB oil content using PCA–MLP method.

The performance of FFB OC model, generated through PCA–MLP method, is demonstrated by the correlation results between laboratory measurements and model predictions of oil content in FFB. Upon calibration, the model's R^2 result is 0.773 (Fig. 9a), while on validation the model's R^2 is 0.7661 (Fig. 9b). In summary, the PCA–MLP model for predicting FFB oil content is presented in Table 6. Compared to FS-MLR model, the FFB OC model performance in this method (PCA–MLP) is somewhat less accurate, possibly due to the application of PCA in reducing spectral reflectance variables, which causes information from the data becomes less detailed. Classification of spectral reflectance data into four principal components is contrasted to the stepwise method that allows the selection of a wider spectral reflectance variables, allowing the model built with more detailed information, and thus performed better. The parameter of FFB OC model, established by means of PCA and MLP methods, is described in the Table 7.

Table 5
Oil content (OC) model predictors and correlated coefficients.

No.	1	2	3	4	5	6	7	8	9	10	11	12	13	14	15	16	Intercept
Coefficients	1.50	−1.57	−5.04	−3.27	−2.14	5.51	−6.33	−5.24	7.41	1.88	2.48	−3.49	−1.40	0.62	−1.12	0.37	25.06
λ (nm)	440	470	480	510	610	690	720	750	760	880	900	910	940	980	990	1000	

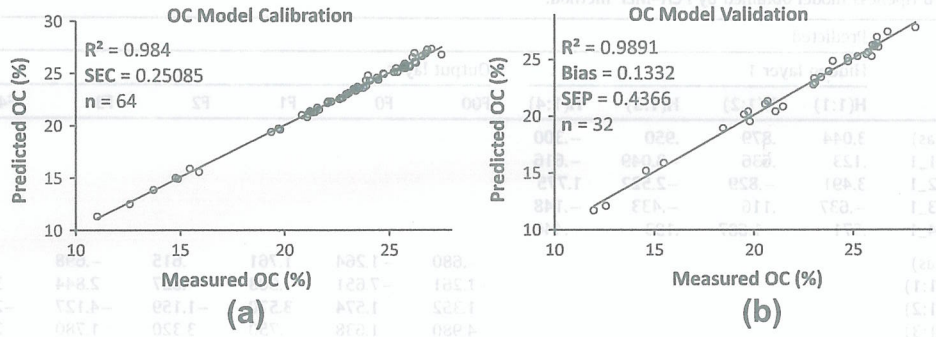

Fig. 7. (a) Calibration and (b) validation results for oil palm FFB oil content (OC) prediction model using FS-MLR method with 16 predictors.

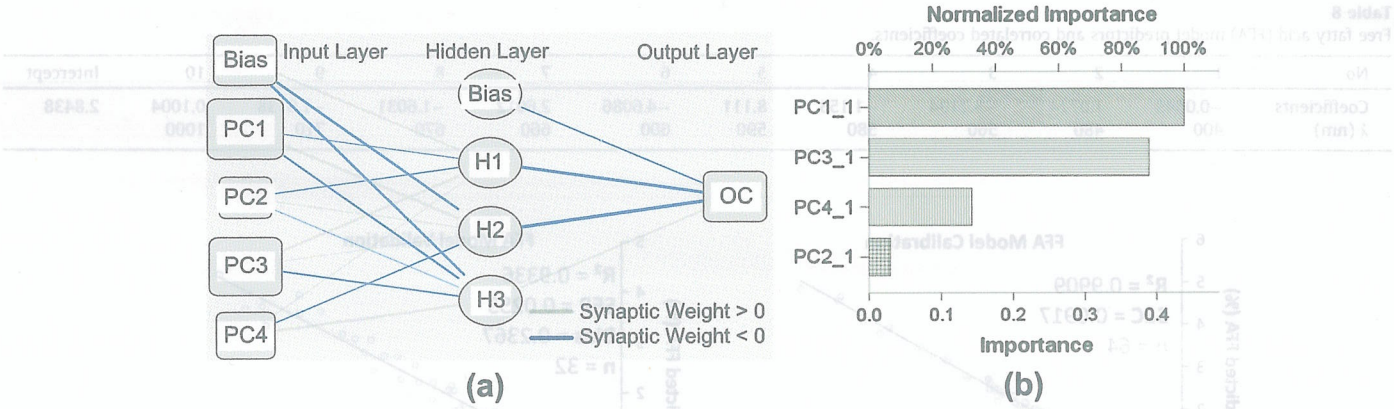

Fig. 8. (a) PCA–MLP diagram of FFB OC model, and (b) model's predictor importance.

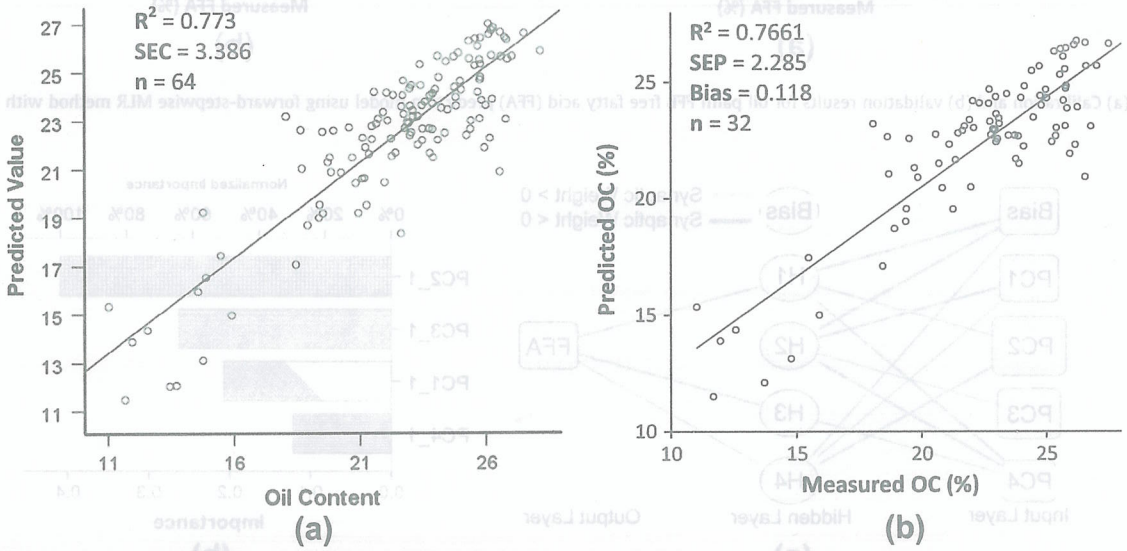

Fig. 9. (a) Calibration and (b) validation results for oil palm FFB oil content (OC) prediction model using PCA–MLP method with 4 principal components.

Table 6
PCA–MLP model performance summary for FFBs oil content prediction.

Training	
Sum of squares error	9.625
Relative error	.219
R^2	0.773
SEC	3.386
n	64
Stopping rule used	1 Consecutive step(s) with no decrease in error[a]
Testing	
Sum of squares error	4.277
Relative error	.253
R^2	0.766
SEP	2.285
Bias	0.118
n	32

[a] Error computations are based on the testing sample.

Table 7
Parameter estimates of FFB OC model (PCA–MLP method).

Predictor		Predicted			
		Hidden layer 1		Output layer	
		H(1:1)	H(1:2)	H(1:3)	Oil content
Input layer	(Bias)	.402	−.668	−.642	
	PC1_1	−.113	.834	−.328	
	PC2_1	−.163	.139	−.081	
	PC3_1	.743	.083	−.223	
	PC4_1	.130	−.167	.823	
Hidden layer 1	(Bias)				−.213
	H(1:1)				−.980
	H(1:2)				−1.480
	H(1:3)				.349

3.3. Modeling FFBs FFA

3.3.1. FS-MLR method for FFB FFA prediction

FFA in oil palm FFB is formed due to fat hydrolysis process, where fat in the oil deteriorates and releases the FFA from triglycerides. This process develops progressively in over ripe bunches (Ismail and Razali, 2010) or when the bunch experiences long delay to be processed in mill. Although fruits' maturity in the bunch is not uniform, the level of FFA is mostly uniform throughout the bunch. High level of FFA is commonly found in over ripe or rotten bunch as well as bruised or injured bunch (Hadi et al., 2009).

Table 8
Free fatty acid (FFA) model predictors and correlated coefficients.

No	1	2	3	4	5	6	7	8	9	10	Intercept
Coefficients	−0.0549	1.0774	−3.2194	−1.153	8.111	−4.6086	2.6012	−1.6031	−1.0138	0.1004	2.8438
λ (nm)	400	480	560	580	590	600	660	670	710	1000	

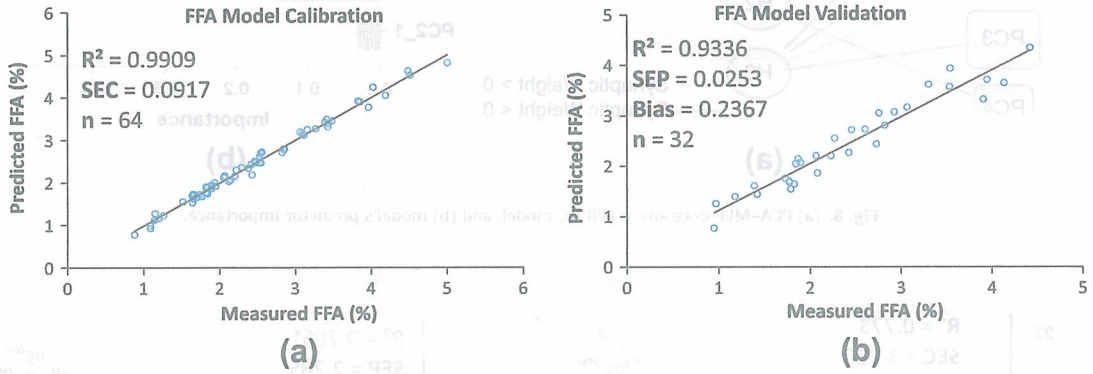

Fig. 10. (a) Calibration and (b) validation results for oil palm FFB free fatty acid (FFA) prediction model using forward-stepwise MLR method with 10 predictors.

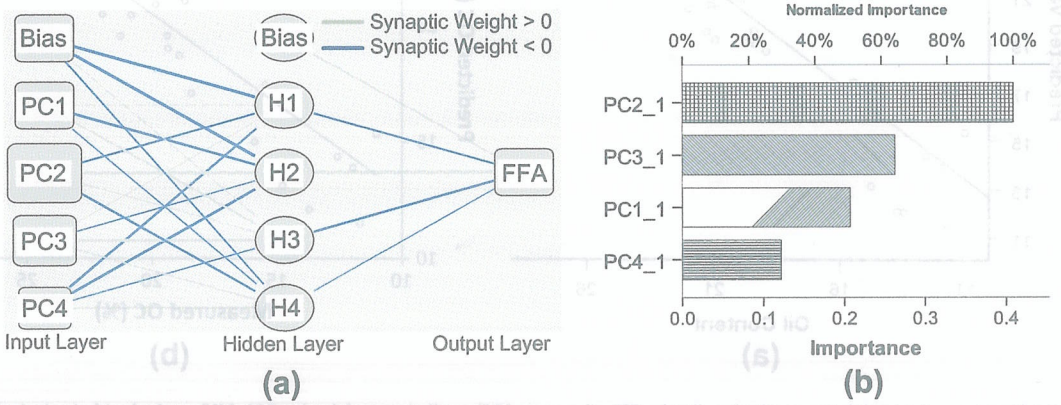

Fig. 11. (a) PCA–MLP diagram of FFB FFA model, and (b) model's predictor importance.

To obtain appropriate model for predicting FFA level in the samples, two methods were used for models creation, the FS-MLR and PCA–MLP. Similarly to the previous sections, the number of variables to be included was taken into consideration to reduce noise influence on the model.

For model creation using FS-MLR method, optimum numbers of predictors for highest R^2 were obtained as 10, with a constant term. The FFA model can be written as:

$$\text{FFA } \% = a + a_1\lambda_1 + a_2\lambda_2 + a_3\lambda_3 + \ldots + a_{10}\lambda_{10} \quad (11)$$

where FFA% is FFA prediction value, a is constant term, a_n is coefficient of nth predictor, and λ_n is the pre-treated reflectance value of the nth predictor. Coefficients for every predictor and the constant term used in the model are shown in Table 8.

The predictors included in this FFA model are pre-treated reflectance data at wavelength of 400, 480, 560, 580, 590, 600, 660, 670, 710 and 1000 nm. The variables in the model suggest that significant differences in oil content in the fruits can be determined by using reflectance at these wavelengths.

In relation to the chlorophyll in the fruits, the model suggests that there is a correlation between fruit's FFA with chlorophyll-a with its second peak absorbance within 660 nm to 670 nm although it is not significant. For the carotenes, model shows no correlation between the carotenes to the wavelengths selected in the model.

The model provides acceptable performance both on calibration and validation (Fig. 10), with R^2 of 0.9909 and SEC of 0.0917 for calibration. In validation, model obtains R^2 of 0.9336 and SEP of 0.2367. The model is considered appropriate since its R^2 values both in calibration and validation are high, while SEC and SEP values are low. Variation in regression coefficients with predictors' wavelength for FFA prediction is shown in Table 8, where peak was observed at around 590 nm corresponding to the orange color.

3.3.2. PCA–MLP method for FFB FFA prediction

The second model of FFA is created using PCA–MLP method. Four principal components are used as predictor variables for the model. Utilizing the statistical software, model employs feed-forward neural network analysis. The network diagram (Fig. 11a) consists of five nodes on input layer, i.e. four principal components and one bias, as source neurons. The hidden layer comprises of four arbitrary variables and one bias, while the output layer only had one node, providing output for FFB FFA prediction. Principal component 2, as the most influence predictor variable in the model

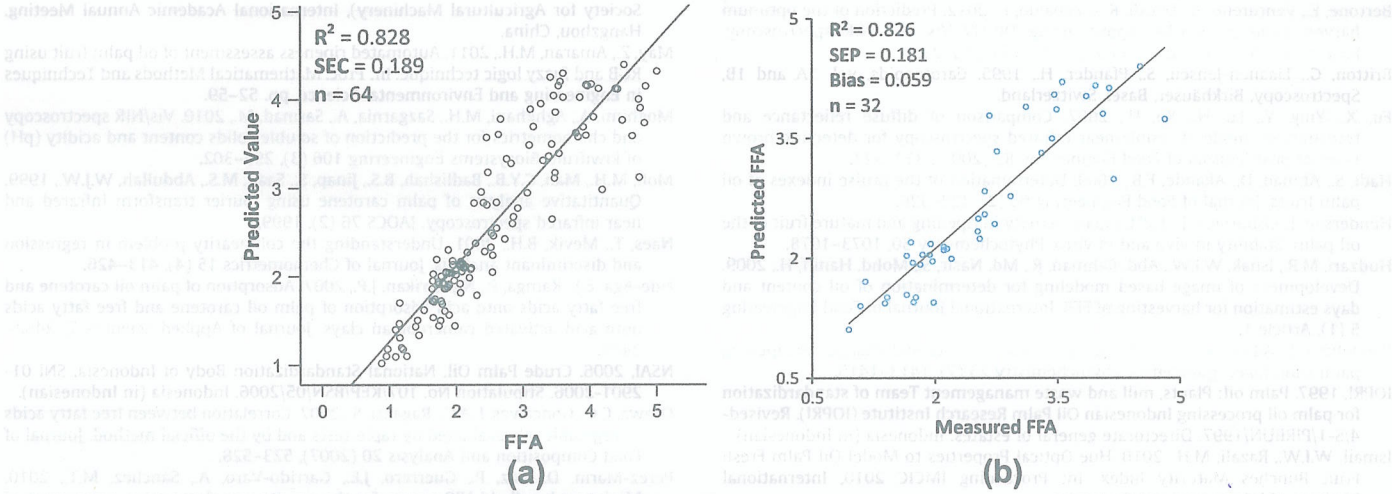

Fig. 12. (a) Calibration and (b) validation results for oil palm FFB free fatty acids prediction model using PCA–MLP method with 4 principal components.

Table 9
PCA–MLP model performance summary for FFBs FFA prediction.

Training	
Sum of squares error	5.359
Relative error	.139
R^2	0.828
SEC	0.189
n	64
Stopping rule used	1 Consecutive step(s) with no decrease in error[a]
Testing	
Sum of squares error	5.062
Relative error	.232
R^2	0.826
SEP	0.181
Bias	0.059
n	32

[a] Error computations are based on the testing sample.

Table 10
Parameter estimates of FFB FFA model (PCA–MLP method).

Predictor		Predicted				
		Hidden layer 1				Output layer
		H(1:1)	H(1:2)	H(1:3)	H(1:4)	FFA
Input layer	(Bias)	−.657	−.982	.039	−.266	
	PC1_1	.023	−.430	.404	−.187	
	PC2_1	−.353	1.147	.040	−.424	
	PC3_1	.092	−.189	.517	.199	
	PC4_1	−.421	−.497	−.256	.261	
Hidden layer 1	(Bias)					.318
	H(1:1)					−.381
	H(1:2)					1.278
	H(1:3)					−.455
	H(1:4)					−.172

(Fig. 11b), represents spectral variable wavelength of 570–700 nm. The wavelength region indicates that chlorophyll influenced FFA model analysis in PCA–MLP method.

Model performs similarly on calibration (R^2 = 0.828) (Fig. 12a), and upon validation (R^2 = 0.826) (Fig. 12b). However, overall performances of the model (Table. 9) are below par when compared to similar model obtained through FS-MLR method (Fig. 10). The summary of PCA–MLP model for predicting FFB free fatty acids is presented in Table 10.

4. Conclusion

In this study, a VIS/NIR spectroscopy technique was employed to estimate ripeness, oil content, and free fatty acid of oil palm FFB, using spectral reflectance and chemical analysis, from 96 samples of eight ripeness variations. The reflectance data were pre-treated using mean-normalized method with 10 nm interval. To address noise, only reflectances within the wavelength of 400–1000 nm were used. The data sets were then compared to the results of chemical analysis to establish models. Two methods are used for developing models, first by FS-MLR and secondly by PCA–MLP. Forward stepwise is employed to obtain simpler model and to remove collinear variables, and thereby enhancing accuracy and reproducibility. Similarly, the PCA is used to extract four principal components from spectral data. For the FS-MLR method, ripeness prediction model employed nine predictors with performance (R^2) of 0.9688 and SEC of 0.1782 upon calibration and R^2 of 0.9375 and SEP of 0.4258 upon validation. The oil content prediction model consisted of 16 predictors, with calibration performance of R^2 and SEC as 0.984 and 0.25085 respectively, while validation performance of R^2 and SEP as 0.9891 and 0.4366. For FFA prediction, the model employed 10 variables with R^2 and SEC as 0.9909 and 0.0917 respectively, while for validation the R^2 was 0.9336 and SEP was 0.2367. For the PCA–MLP method, ripeness model performances (R^2) are 0.9393 and 0.9351 for calibration and validation respectively, with SEC and SEP of 0.344 and 0.36. On the OC model, the R^2 on calibration and validation are 0.773 and 0.7661 respectively, and SEC and SEP value are 3.386 and 2.285. As for the FFA model, calibration and validation performance (R^2) are 0.828 and 0.826 respectively, while the SEC and SEP are obtained as 0.189 and 0.181. Overall, the models created using FS-MLR methods performed better, due to more predictor variables employed.

Acknowledgements

The research was supported by the Asian Institute of Technology, (Thailand) and the General Directorate of Higher Education (DIKTI), (Indonesia). The authors would like to also acknowledge support received from the Indonesian Oil Palm Company (PTPN VIII).

References

AOCS, 2004, Official methods and recommended practices of the American Oil Chemists Society. Sampling and analysis of commercial fats and oil. American Oil Chemists Society, Champaign, USA.

Bertone, E., Venturello, A., Leardi, R., Geobaldo, F., 2012. Prediction of the optimum harvest time of 'Scarlet' apples using DR-UV-Vis and NIR spectroscopy. Postharvest Biology and Technology 69 (2012), 15–23.
Britton, G., Liaanen-Jensen, S., Pfander, H., 1995. Carotenoids, vol. 1A and 1B, Spectroscopy, Birkhäuser, Basel, Switzerland.
Fu, X., Ying, Y., Lu, H., Xu, H., 2007. Comparison of diffuse reflectance and transmission mode of visible-near infrared spectroscopy for detecting brown heart of pear. Journal of Food Engineering 83 (2007), 317–323.
Hadi, S., Ahmad, D., Akande, F.B., 2009. Determination of the bruise indexes of oil palm fruits. Journal of Food Engineering 95 (2), 322–326.
Henderson, J., Osborne, K.J., 1991. Lipase activity in ripening and mature fruit of the oil palm. Stability in vivo and in vitro. Phytochemistry 30, 1073–1078.
Hudzari, M.R., Ishak, W.I.W., Abd. Rahman, R., Md. Nasir, S., Mohd. Haniff, H., 2009. Development of image based modeling for determination of oil content and days estimation for harvesting of FFB. International Journal of Food Engineering 5 (1). Article 1.
Ikemefuna, J., Adamson, I., 1984. Chlorophyll and carotenoid changes in ripening palm fruit, Elaeis guineensis. Phytochemistry 23 (7), 1413–1415.
IOPRI, 1997. Palm oil: Plants, mill and waste management Team of standardization for palm oil processing Indonesian Oil Palm Research Institute (IOPRI). Revised-4/S-1/PIRBUN/1997. Directorate general of estates. Indonesia (in Indonesian).
Ismail, W.I.W., Razali, M.H., 2010. Hue Optical Properties to Model Oil Palm Fresh Fruit Bunches Maturity Index. In: Proceeding IMCIC 2010, International Institute of Informatics and Systemics.
Jolliffe I.T., 2002. Principal Component Analysis, Series: Springer Series in Statistics, second ed., Springer, NY, 2002, XXIX, 487 p. ISBN 978-0-387-95442-4.
Kaiser, H.F., 1960. The application of electronic computers to factor analysis. Educational and Psychological Measurement 20, 141–151.
Keshvadi, A., Endan, J.B., Harun, H., Ahmad, D., Saleena, F., 2011. The effect of surface color on palm oil quality during the ripening process of fresh fruits. Journal of Food, Agriculture & Environment 9 (3–4), 61–67.
Liu, Y., Chen, X., Ouyang, A., 2008. Nondestructive determination of pear internal quality indices by visible and near-infrared spectrometry. LWT – Food Science and Technology 41 (2008), 1720–1725.
Louw, E.D., Theron, K.I., 2010. Robust prediction models for quality parameters in Japanese plums (*Prunus salicina* L.) using NIR spectroscopy. Postharvest Biology and Technology 58 (3), 176–184.
Magwaza, L.S., Opara, U.L., Terry, L.A., Landahl, S., Cronje, P.J., Nieuwoudt, H., Mouazen, A.M., Saeys, W., Nicolai, B.M., 2012. Prediction of 'Nules Clementine' mandarin susceptibility to rind breakdown disorder using Vis/NIR spectroscopy. Postharvest Biology and Technology 74 (2012), 1–10.
Makky, M., Herodian, S., Subrata, I.D.M., 2004. Design and technical test of visual sensing system for palm oil harvesting robot. International Seminar on Advanced Agricultural Engineering and Farm Work Operation. Bogor, Indonesia. Proc. pp. 582–592.
Makky, M., Soni, P., 2013a. Development of an automatic grading machine for oil palm fresh fruit bunches (FFBs) based on machine vision. Computers and Electronics in Agriculture 93 (2013), 129–139.
Makky, M., Soni, P., 2013b. Towards sustainable green production: exploring automated Grading for oil palm fresh fruit bunches (FFB) using machine vision and spectral analysis. International Journal on Advanced Science, Engineering and Information Technology 3 (1), 1–7, ISSN: 2088-5334.
Makky, M., Soni, P., Salokhe, V.M., 2012. Machine vision application in indonesian oil palm industry. In: Proceedings of the Asian Forum of 2012 CSAM (Chinese Society for Agricultural Machinery), International Academic Annual Meeting. Hangzhou, China.
May, Z., Amaran, M.H., 2011. Automated ripeness assessment of oil palm fruit using RGB and fuzzy logic technique. In: Proc. Mathematical Methods and Techniques in Engineering and Environmental Science, pp. 52–59.
Moghimi, A., Aghkhani, M.H., Sazgarnia, A., Sarmad, M., 2010. Vis/NIR spectroscopy and chemometrics for the prediction of soluble solids content and acidity (pH) of kiwifruit. Biosystems Engineering 106 (3), 295–302.
Moh, M.H., Man, C.Y.B., Badlishah, B.S., Jinap, S., Saad, M.S., Abdullah, W.J.W., 1999. Quantitative analysis of palm carotene using fourier transform infrared and near infrared spectroscopy. JAOCS 76 (2), 1999.
Naes, T., Mevik, B.H., 2001. Understanding the collinearity problem in regression and discriminant analysis. Journal of Chemometrics 15 (4), 413–426.
Nde-Aga, B.J., Kamga, P., Nguetrikan, J.P., 2007. Adsorption of palm oil carotene and free fatty acids onto acid adsorption of palm oil carotene and free fatty acids onto acid activated cameroonian clays. Journal of Applied Sciences 7, 2462–2467.
NSAI, 2006. Crude Palm Oil. National Standardization Body of Indonesia. SNI 01-2901-2006. Stipulation No. 107/KEP/BSN/05/2006. Indonesia (in Indonesian).
Osawa, C.C., Goncalves, L.A.G., Ragazzi, S., 2007. Correlation between free fatty acids of vegetable oils evaluated by rapid tests and by the official method. Journal of Food Composition and Analysis 20 (2007), 523–528.
Pérez-Marín, D., Paz, P., Guerrero, J.E., Garrido-Varo, A., Sánchez, M.T., 2010. Miniature handheld NIR sensor for the on-site non-destructive assessment of post-harvest quality and refrigerated storage behavior in plums. Journal of Food Engineering 99 (3), 294–302.
Saeed, O.M.B., Sankaran, S., Shariff, A.R.M., Shafri, H.Z.M., Ehsani, R., Alfatni, M.S., Hazir, M.H.M., 2012. Classification of oil palm fresh fruit bunches based on their maturity using portable four-band sensor system. Computers and Electronics in Agriculture 82 (2012), 55–60.
Shao, Y., He, Y., Gómez, A.H., Pereir, A.G., Qiu, Z., Zhang, Y., 2007. Visible/near infrared spectrometric technique for nondestructive assessment of tomato 'Heatwave' (Lycopersicum esculentum) quality characteristics. Journal of Food Engineering 81, 672–678.
Sinelli, N., Spinardi, A., Egidio, V.D., Mignani, I., Casiraghi, E., 2008. Evaluation of quality and nutraceutical content of blueberries (*Vaccinium corymbosum* L.) by near and mid-infrared spectroscopy. Postharvest Biology and Technology 50 (1), 31–36.
Sirisomboon, P., Tanaka, M., Kojima, T., Williams, P., 2012. Nondestructive estimation of maturity and textural properties on tomato 'Momotaro' by near infrared spectroscopy. Journal of Food Engineering 112 (3), 218–226.
Streitweiser, H., 1981. Introduction to Organic Chemistry. MacMillan, New York, USA.
Subedi, P.P., Walsh, K.B., Owens, G., 2007. Prediction of mango eating quality at harvest using short-wave near infrared spectrometry. Postharvest Biology and Technology 43 (3), 326–334.
Valous, N.A., Mendoza, F., Sun, D.W., 2010. Emerging noncontact imaging, spectroscopic and colorimetric technologies for quality evaluation and control of hams: a review. Trends in Food Science & Technology 21 (2010), 26–43.
Wang, J., Nakano, K., Ohashi, S., Takizawa, K., He, J.G., 2010. Comparison of different modes of visible and near-infrared spectroscopy for detecting internal insect infestation in jujubes. Journal of Food Engineering 101 (2010), 78–84.

Journal of Food Engineering

Country	United Kingdom
Subject Area and Category	Agricultural and Biological Sciences Food Science
Publisher	Elsevier BV
Publication type	Journals
ISSN	02608774
Coverage	1982-ongoing
Scope	The journal publishes original research and review papers on any subject at the interface between food and engineering, particularly those of relevance to industry, including: Engineering properties of foods, food physics and physical chemistry; processing, measurement, control, packaging, storage and distribution; engineering aspects of the design and production of novel foods and of food service and catering; design and operation of food processes, plant and equipment; economics of food engineering, including the economics of alternative processes. Accounts of food engineering achievements are of particular value. (source)

116

H Index

Quartiles

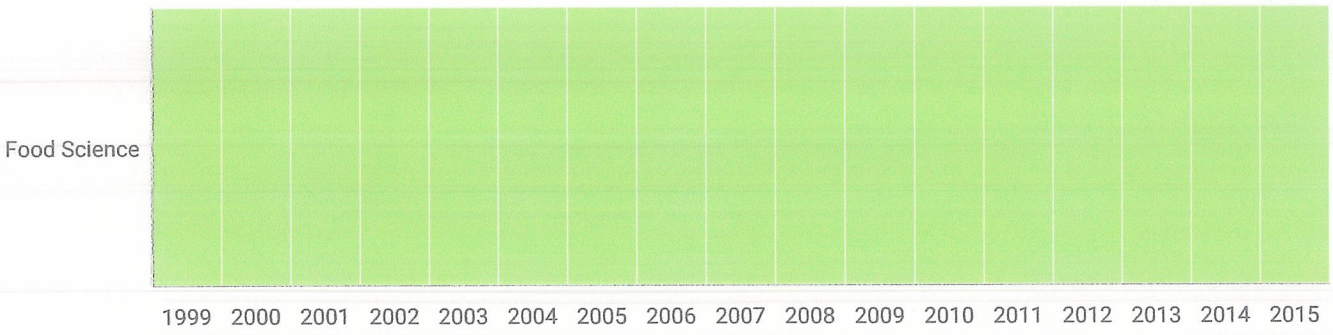

SJR

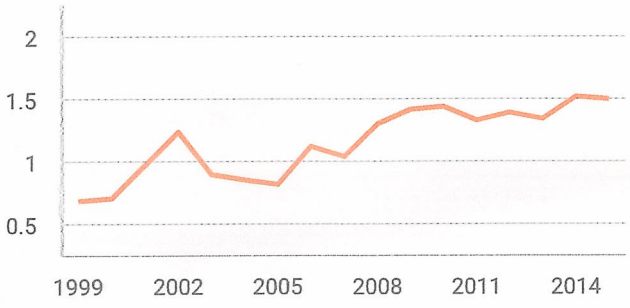

Citations per document

Total Cites Self-Cites

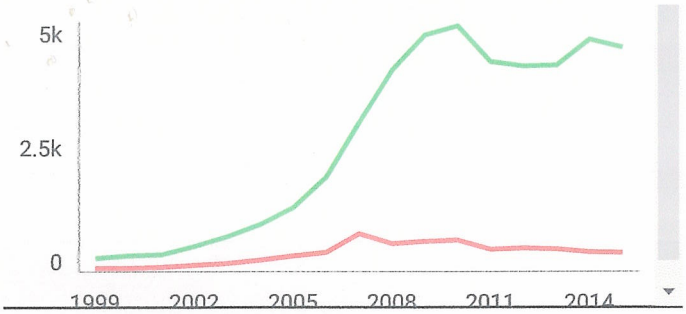

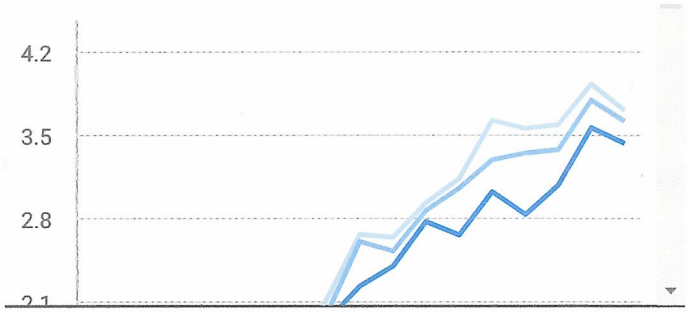

External Cites per Doc Cites per Doc

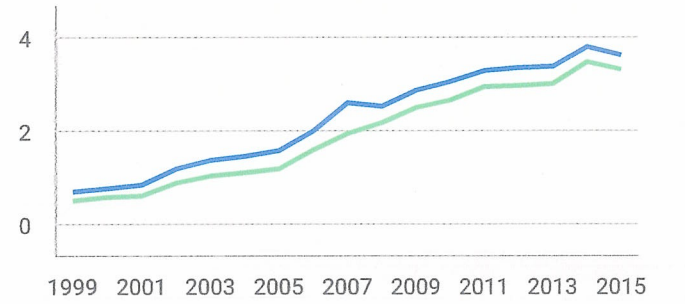

% International Collaboration

Citable documents Non-citable documents

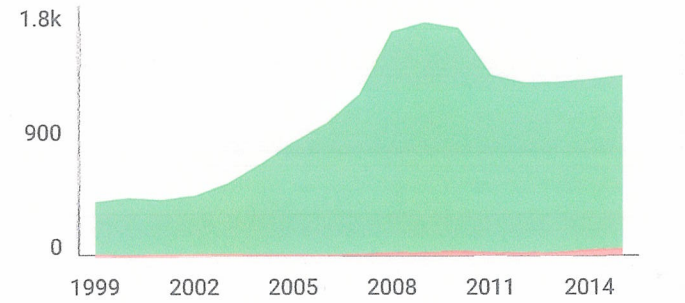

Cited documents Uncited documents

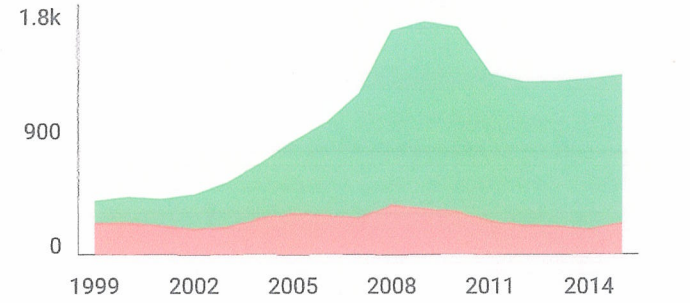

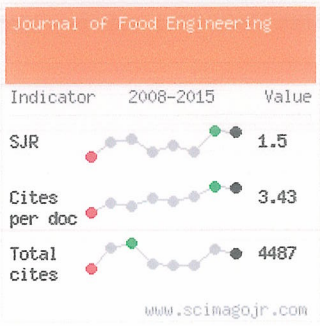

← Show this widget in your own website

Just copy the code below and paste within your html code:

```
<a href="http://www.scimagc
```

Developed by:

Powered by:

Volume 120, Issue 1, January 2014

ISSN 0260-8774

ELSEVIER

journal of food engineering

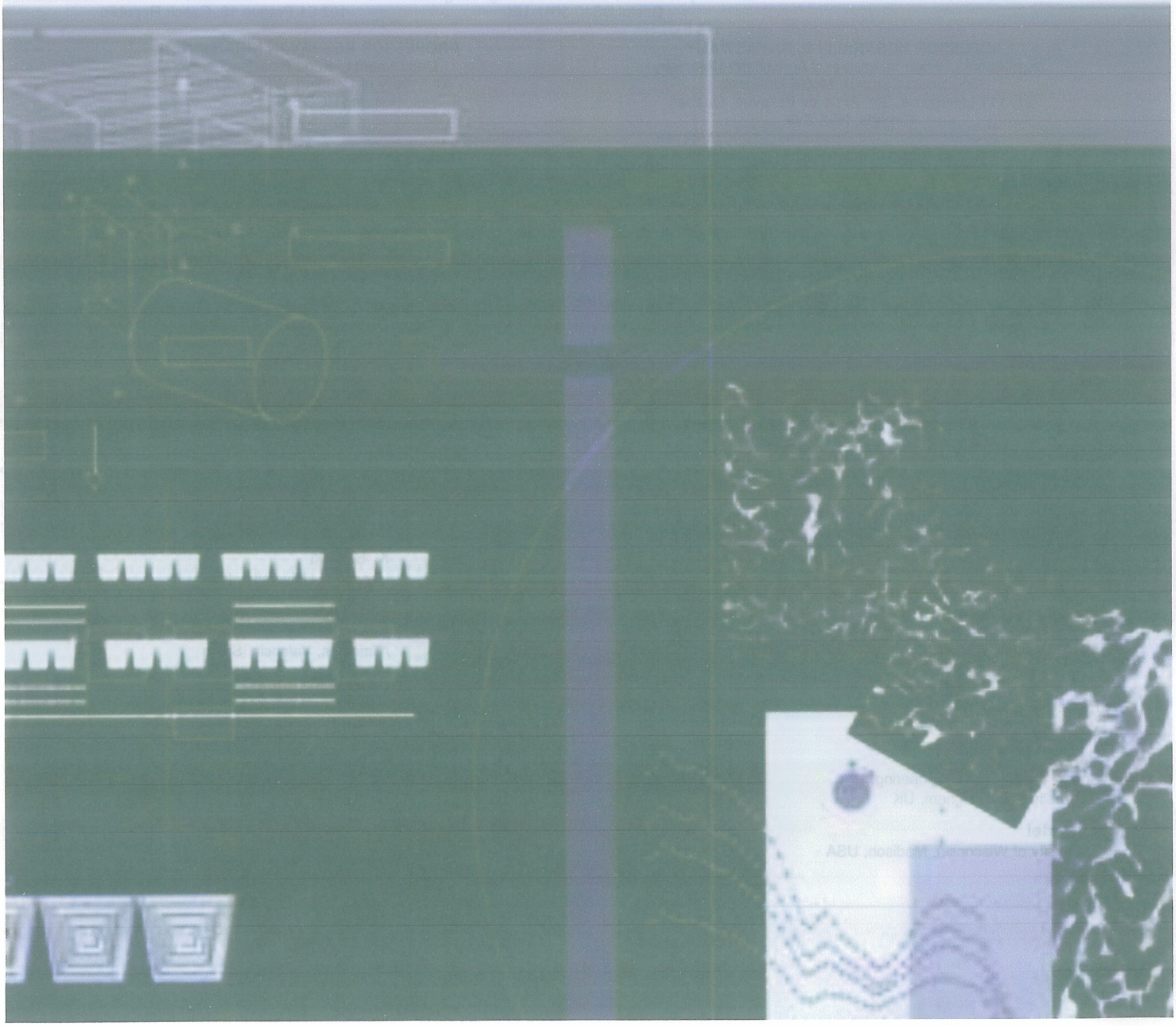

JOURNAL OF FOOD ENGINEERING

The journal publishes original research and review papers on any subject at the interface between food and engineering, particularly those of relevance to industry, including:

- engineering properties of foods, food physics and physical chemistry;
- processing, measurement, control, packaging, storage and distribution;
- engineering aspects of the design and production of novel foods and of food service and catering;
- design and operation of food processes, plant and equipment;
- economics of food engineering, including the economics of alternative processes.

Accounts of food engineering achievements are of particular value.

Printed in the Netherlands

Journal of Food Engineering

ISSN: 0260-8774

Editor-in-Chief: R.P. Singh

Journal of Food Engineering is an official scientific journal of the International Society of Food Engineering (ISFE).

Journal Metrics

- **Five-Year Impact Factor (2014): 3.216**

  To calculate the five year Impact Factor, citations are counted in 2014 to the previous five years and divided by the source items published in the previous five years.

  Published by Thomson Reuters

The journal publishes original research and review papers on any subject at the interface between **food** and **engineering**, particularly those of relevance to industry, including:

Engineering properties of foods, **food physics** and **physical chemistry**; processing, measurement, control, packaging, storage and distribution; engineering aspects of the design and production of **novel foods** and of food service and **catering**; design and operation of **food processes**, plant and **equipment**; **economics** of food engineering, including the economics of alternative processes.

Accounts of food engineering achievements are of particular value.

Benefits to authors

We also provide many author benefits, such as free PDFs, a liberal copyright policy, special discounts on Elsevier publications and much more. Please click here for more information on our author services.

Please see our Guide for Authors for information on article submission. If you require any further information or help, please visit our support pages: http://support.elsevier.com

Journal of Food Engineering

ISSN: 0260-8774

Editor-in-Chief: R.P. Singh

Abstracting and Indexing

- SCOPUS
- ADONIS
- AGRICOLA
- BIOSIS
- Cambridge Scientific Abstracts
- Chemical Abstracts
- Chemical Engineering Biotechnology Abstracts
- Current Contents/Agriculture, Biology & Environmental Sciences
- Engineering Abstracts
- Engineering Index
- FSTA (Food Science and Technology Abstracts)
- Process and Chemical Engineering
- Research Alert
- SCISEARCH
- Science Citation Index
- EMBiology

Journal of Food Engineering
ISSN: 0260-8774

Editorial Board

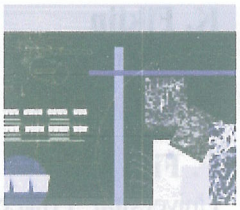

Journal of Food Engineering

ISSN: 0260-8774

Volume 120, Pages 1-276
January 2014

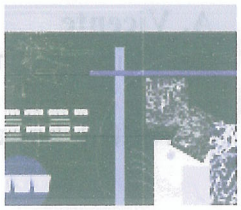

Articles 1 - 33

Highlights: An algorithm for inspecting a small and minute crack in biscuit products was proposed using machine vision technology; A spatial pyramid approach was used to construct multi-resolution image; An advanced image enhancement and recursive Canny–Deriche filter were developed; A new unimodal thresholding technique was investigated for crack segmentation; The detection is achieved by means of pyramid SVM featuring Wilk's λ selection criteria.

31. **In situ quality assessment of intact oil palm fresh fruit bunches using rapid portable non-contact and non-destructive approach**

Muhammad Makky, Peeyush Soni

Highlights: Rapid and non-destructive examination for oil palm FFB quality inspection; VIS/NIR spectroscopy for field application; The best models accuracy was 96.88% for ripeness prediction, 98.4% for oil content prediction, and 99.1% for free fatty acid prediction.

32. **Technological properties and enhancement of antifungal activity of a *Paeonia rockii* extract encapsulated in a chitosan-based matrix**

Francesca Sansone, Patrizia Picerno, Teresa Mencherini, Amalia Porta, Maria Rosaria Lauro, Paola Russo, Rita Patrizia Aquino

Highlights: Microencapsulation of *Paeonia rockii* extract (PPR) in a spray dried chitosan (C) matrix; 0.5% w/v C and 1/1 C/PPR ratio led to high process yields (70.1%); The microencapsulation process led to high encapsulation efficiency (82.4%) and low dimensional distribution (5.15 μm); The produced powder (C-PPR) showed enhanced water dissolution properties and storage stability with respect to PPR; C-PPR exhibited antioxidant property and enhanced antifungal activity against *Candida albicans* with respect to PPR.

33. **Radiofrequency disinfestation treatments for dried fruit: Model development and validation**

Bandar Alfaifi, Juming Tang, Yang Jiao, Shaojin Wang, Barbara Rasco, Shunshan Jiao, Shyam Sablani

Highlights: A COMSOL simulation model was developed and validated experimentally; RF Heating uniformity of raisins in a rectangular container was determined; Simulated and experimental temperatures were highest in the middle layer; Corners and edges received more RF heat than the centers in each layer; UI was most affected by dielectric properties & electrode voltage.
